Binaural beats through the auditory pathway: from brainstem to connectivity patterns

Hector D. Orozco Perez, Guillaume Dumas, Alexandre Lehmann

eNeuro

Research Article: New Research | Cognition and Behavior

Binaural beats through the auditory pathway: from brainstem to connectivity patterns

https://doi.org/10.1523/ENEURO.0232-19.2020

Cite as: eNeuro 2020; 10.1523/ENEURO.0232-19.2020

Received: 18 June 2019
Revised: 23 December 2019
Accepted: 20 January 2020

Binaural beats through the auditory pathway: from brainstem to connectivity patterns

Abbreviated Title: Binaural Beats through the auditory pathway

Hector D Orozco Perez[1,2], Guillaume Dumas[3,4] and Alexandre Lehmann[1,5,6]

[1] Laboratory for Brain, Music and Sound Research (BRAMS), Montreal, Canada (H2V 2S9).

[2] McMaster University, Department of Psychology, Neuroscience and Behavior, Hamilton, Canada (L8S 4L8).

[3] Human Genetics and Cognitive Functions, Institut Pasteur, UMR3571 CNRS, Université de Paris, Paris, France (75015).

[4] Center for Complex Systems and Brain Sciences, Florida Atlantic University, Boca Raton, FL, USA (FL 33431).

[5] Department of Otolaryngology Head & Neck Surgery, McGill University, Montreal, Canada (H3A 0G4).

[6] Centre for Research on Brain, Language and Music (CRBLM), Montreal, Canada (H3G 2A8).

Author contributions: HO, AL, and GD designed research; HO and AL performed research; GD contributed analytic tools; HO and GD analyzed data, HO wrote the paper; AL and GD provided edits and comments for the paper.

Correspondence should be addressed to hector.dom.orozco@gmail.com

Acknowledgements: The authors of this paper would like to thank Pierre Rainville and Bérangère Houze for sharing the E-SAS scales; Mihaela Felezeu for all the help and support during data acquisition; and our participants for volunteering their time to perform the experiment.

Authors report no conflict of interest

Funding sources: GD was financially supported by the Institut Pasteur

Abstract

Binaural beating is a perceptual auditory illusion occurring when presenting two neighboring frequencies to each ear separately. Several controversial claims have been attributed to binaural beats regarding their ability to entrain human brain activity and mood, in both the scientific literature and the marketing realm. Here, we sought to address those questions in a robust fashion using a single-blind, active-controlled protocol. To do so, we compared the effects of binaural beats with a control beat stimulation (monaural beats, known to entrain brain activity but not mood) across four distinct levels in the human auditory pathway: subcortical and cortical entrainment, scalp-level Functional Connectivity and self-reports. Both stimuli elicited standard subcortical responses at the pure tone frequencies of the stimulus (i.e., Frequency Following Response), and entrained the cortex at the beat frequency (i.e., Auditory Steady State Response). Furthermore, Functional Connectivity patterns were modulated differentially by both kinds of stimuli, with binaural beats being the only one eliciting cross-frequency activity. Despite this, we did not find any mood modulation related to our experimental manipulation. Our results provide evidence that binaural beats elicit cross frequency connectivity patterns, but weakly entrain the

cortex when compared to monaural beat stimuli. Whether binaural beats have an impact on cognitive performance or other mood measurements remains to be seen and can be further investigated within the proposed methodological framework.

Visual Abstract

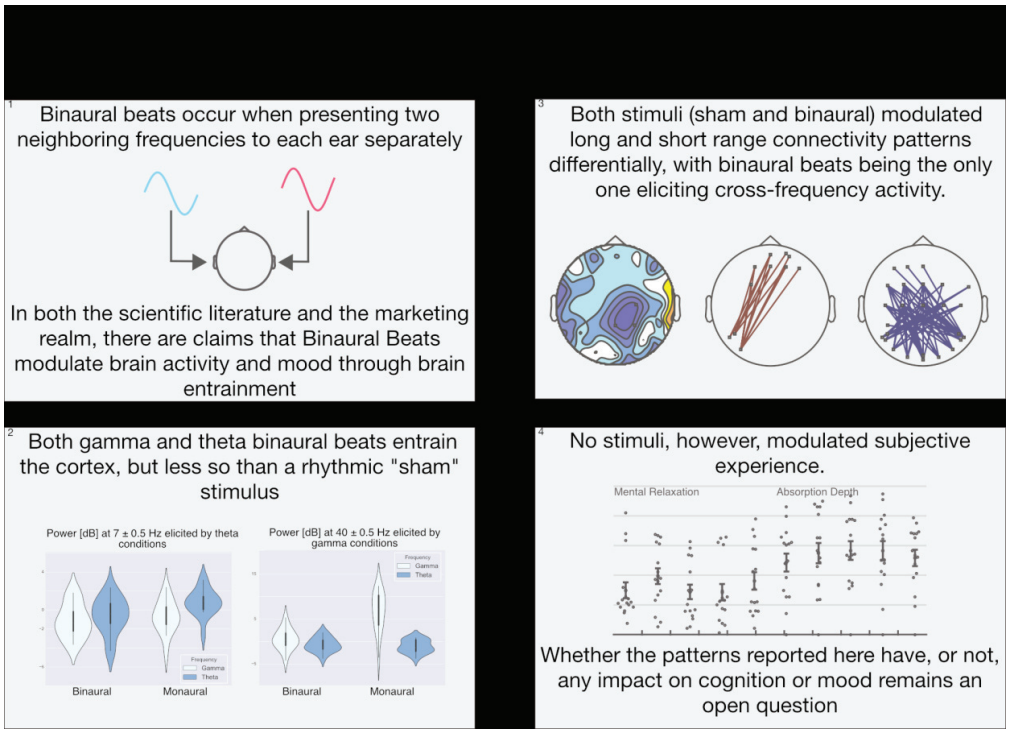

Significance Statement

Binaural beats have been a source of speculation and debate in the scientific community. Our study addresses controversial claims and approaches them using proper experimental control and

55 modern signal processing techniques. Here we show that binaural beats can both entrain the
56 cortex and elicit specific connectivity patterns. Regardless of this, our monaural control condition
57 was able to entrain the cortex more strongly, and both binaural beats and the control condition
58 failed to regulate mood. All in all, though binaural beats entrain cortical activity and elicit complex
59 patterns of connectivity, the functional significance (if any) of binaural beats, and whether they are
60 more "special" than monaural beats remain open questions.
61

62 # Introduction

63 Humans use music and rhythm as mood enhancers. Be it in social gatherings or late study nights,
64 we use audio stimuli to set the "right mood" and improve our cognitive performance
65 (Mammarella et al., 2007; Schellenberg et al., 2007; Tarr et al., 2014). Binaural beats, an auditory
66 illusion that occurs when presenting two similar pure tones to each ear separately, have been
67 purported to induce mood alterations, contingent upon the beat frequency. Claims range from
68 entraining the whole brain (Atwater, 2004; Rhodes, 1993), to altering states of consciousness (I-
69 Doser, accessed May 2018; Atwater, 1997). The possibility of binaural beats modulating cognitive
70 states without prior training makes them an interesting candidate for cost-effective applications in
71 both healthy and impaired populations.

Presenting two tones with a slight frequency mismatch to each ear separately creates a perception of a third tone, a binaural beat, that oscillates at the absolute difference between the tones (Oster, 1973; Moore, 2012). These beats are thought to originate subcortically in the medial nucleus of the superior olivary complex, the first nucleus in the auditory pathway to receive bilateral input (Wernick & Starr, 1968; Kuwada & Wickesberg, 1979). This "illusory" third tone is lateralized between the left and right ear of the listener, making binaural beats useful for spatial sound research (Ross et al., 2014). Binaural beats can entrain cortical activity at both the specific frequency of the beat (Pratt et al., 2010) and cross-frequency modulations, such as theta beats driving interhemispheric alpha synchronization (Solcà et al., 2016). They also seem to modulate mood (Wahbeh et al., 2007), pain perception (Zampi, 2015) and cognitive performance in memory tasks (Kennerly, 1994). The cognitive effects of binaural beats are attributed to their capacity to drive neural oscillations at the beat frequency through differential hemispheric synchronization frequencies. The reported cognitive modulations, however, appear inconsistent and seem to depend on several mediating factors, such as frequency of stimulation, differing exposure time and stimuli masking (Garcia-Argibay et al., 2018). Furthermore, no study to date has fully characterized binaural beats throughout the auditory pathway (from subcortical responses to Functional Connectivity) and compared their effect to that of a non-binaural rhythmic control (i.e., monaural beats, created by digitally summing each tone before presentation). Indeed, monaural beats readily entrain the cortex to specific frequencies (Nozaradan et al., 2016), and repetitive and

rhythmic stimuli (such as mantras or tones) are widely used in contemplative and religious practices with positive physiological impact (Bernardi et al., 2001; Bernardi et al., 2017). It remains open questions whether the reported effects of binaural beats are due to: (1) their asymmetrically driven rhythmicity (the binaural aspect is essential to their effectiveness), (2) their capability of entraining brain oscillations (as would also be the case with monaural beats) or (3) a placebo effect. To address these, we recorded electroencephalography (EEG) during a single-blind, active-controlled task in which participants listened to both binaural and monaural beats.

Our main objective was to characterize brain responses and cognitive alterations induced by binaural beats, compared to a monaural beat control condition. Our secondary objective was to compare the neural and subjective effects elicited by two different beat frequencies. We used theta (7 Hz) beats because they have been associated with reduced anxiety levels (Isik et al., 2017), and gamma beats (40 Hz) because they have been associated with attention modulation (Colzato et al., 2017). Furthermore, these frequencies have been associated with large-scale integration models of the brain (Varela et al., 2001; Canolty and Knight, 2010). We compared responses between binaural and monaural beats at four levels: subcortical entrainment to the carrier tones in the form of a Frequency Following Response (FFR; Skoe & Kraus, 2010), cortical entrainment to the beat in the form of an Auditory Steady State Response (ASSR; Picton et al., 2003), changes in Functional Connectivity using phase-based statistics (Nolte et al. 2004; Lachaux et al., 2000) and

self-reported mood changes using analogue scales (Rainville et al., 2002). We hypothesized both beats would elicit cortical and subcortical responses to the beat (ASSR) and pure tone frequencies (FFR) respectively. However, we expected binaural beats to elicit Functional Connectivity changes and modulate mood, with no such changes during the control condition. We hypothesized that theta beats would facilitate a relaxed state, while gamma beats would elicit a more alert state. By presenting converging evidence from different approaches (self-reports, EEG), we aimed to elucidate whether binaural beats are a special kind of stimulus or reported effects could be achieved with non-binaural rhythmic stimuli.

Materials & Methods

To understand the functional meaning of the entrainment and connectivity patterns associated with binaural beats, we investigated the differences between monaural and binaural beats by comparing subcortical, cortical and subjective responses elicited through a single-blind, passive listening task with a 2x2 factorial design (two within factors: beat type and beat frequency).

Participants

Sixteen participants (nine female, seven male; mean age 27.4±5.5) volunteered for the experiment and provided written informed consent. Exclusion criteria included neurological damage or abnormalities (e.g. demyelination), and major hearing loss (0-20 HL dB) as self-reported by the participants. The experimental procedures conformed to the World Medical Association' s Declaration of Helsinki and were approved by the Research Ethics Committee of the Faculty for Arts and Sciences of the University of Montreal.

Stimuli

Binaural beats entrain cortical activity at the specific frequency of the beat percept (Draganova et al., 2007; Schwarz & Taylor, 2005; Pratt et al., 2010). We refer to beat frequency as the frequency of this percept, which is the difference between the pure tones; either 40 Hz for gamma conditions (380 Hz & 420 Hz) or 7 Hz for theta conditions (396.5 Hz & 403.5 Hz). This rhythmic percept is a key piece of the purported subjective effects of binaural beats in the scientific and pseudo-scientific literature. They claim entrainment to it regulates mood and cognition. To elucidate whether and how binaural beats regulate mood, we chose monaural beats as a control that would rule out rhythmicity as an influencing factor. Binaural beats do not contain the beat frequency in neither their spectrum nor their envelope, but this percept is presumably created in

the medial nucleus of the superior olivary complex (Wernick & Starr, 1968; Kuwada & Wickesberg, 1979). On the other hand, monaural beats do contain it in their envelope (see Figure 1).

Binaural beat stimuli consisted of two pure sine tones with equal starting phase and a slight frequency mismatch presented separately to each ear (Figure 1, Columns 1 and 2). These two pure tones were superimposed digitally (added together and divided by two to control for loudness) to create the monaural control condition, which was presented monaurally to both ears—each ear was presented with the same stimuli (see Becher et al., 2015; Schwarz & Taylor, 2005; and Draganova et al., 2007 for other examples where monaural beats were used as a control condition). By summing both pure tones, we essentially created amplitude-modulated stimuli, which excel at entraining the brain (Ross et al., 2000).

We chose carrier frequencies around 400 Hz for two reasons: best perception of binaural beats occurs at carrier tones between 400 and 500 Hz (Licklider et al., 1950; Perrot & Nelson, 1969) and this frequency range minimizes cortical contributions to the brainstem responses (Coffey et al., 2016). Both kinds of stimuli (binaural and monaural control) were root mean squared normalized. The lower of both frequencies (380 and 396.5 Hz) was always presented to the left ear (i.e., pure tone presentation was not altered between left and right ears).

158 Frequency choice: Theta

159 Auditory stimulation at the theta frequency band (4 - 7 Hz) has been associated with positive
160 emotional experiences and introspection (Aftanas & Golocheikine, 2001), reduced perceived pain
161 in patients with chronic pain (Zampi, 2015), states of meditation and decreased alertness
162 (Jirakittayakorn & Wongsawat, 2017) and enhancement of immediate verbal memory (Ortiz et al.,
163 2008). Furthermore, theta cortical activity is related to concentration, focused attention and a
164 general meditative state (Takahashi et al., 2005; Lagopoulos et al., 2009). We chose theta beat
165 frequency to explore the possibility of eliciting a mindful and relaxed state in the participants.
166

167 Frequency choice: Gamma

168 Auditory gamma stimulation (32 - 48 Hz) has been associated with binaural sound integration
169 (Ross et al., 2014), divergent thinking (Reedijk et al., 2013) and attention control (Reedijk et al.,
170 2015). Furthermore, auditory cortices readily entrain to it (Schwarz & Taylor, 2005; Ross et al.,
171 2014), and it seems to be a "natural frequency" of these areas, even during resting state
172 (Hillebrand et al., 2012). We chose gamma beat frequency to explore the possibility of eliciting a
173 heightened attention cognitive state in the participants.
174

Procedure

Participants started by filling out a general information and music abilities questionnaire. We then fitted a headcap on participants' heads and placed EEG electrodes in it using a conductive gel. The experiment took place in a sound-attenuated, electromagnetically shielded room. Participants were asked to relax their upper body, close their eyes, avoid body movements and to pay attention to the beat throughout the experiment (Schwarz & Taylor., 2005). We recorded data from five experimental blocks: an eight-minute baseline (no stimulus presentation; eyes-closed) followed by the four pseudo-randomized experimental conditions (binaural gamma, monaural gamma, binaural theta, monaural theta), each lasting for eight minutes. After each recording block, participants were asked to rate their experience using two visual analogue scales. They were also given the opportunity to take a break in the middle of the experiment. Auditory stimuli (both binaural and monaural beats) were generated live (i.e. during the recording block) to ensure sub-millisecond phase accuracy using a signal processing system (RX6, Tucker-Davis Technologies, www.tdt.com) controlled with MATLAB software (The Mathworks, www.mathworks.com) and delivered via insert earphones (ER3, Etymotic Research, www.etymotic.com). Auditory stimuli were processed at 48 kHz and were each presented continuously for eight minutes at 70 dB SPL. For the purpose of further analysis and the epoching of continuous data, triggers were sent every

eight seconds via parallel ports using the signal processing system (RX6, Tucker-Davis Technologies, www.tdt.com) and recorded along with the EEG data.

Sound calibration

Output sound from the signal processing system was calibrated to be presented at 70 dB SPL at the level of each ear, using a Sound-Pro sound level meter (model DL 1/3 Octave Datalogging RTA) and a 2-CC ear coupler for insert earphones calibration. Calibration measurements were done using a slow rate mode with an A-weighting frequency filter.

EEG data acquisition

EEG was recorded using 64 active sintered Ag-AgCl electrodes placed on the scalp according to the International 10/10 system (ActiveTwo, Biosemi, The Netherlands). The active electrodes contain the first amplifier stage within the electrode cover and provide impedance transformation on the electrode to prevent interference currents from generating significant impedance-dependent nuisance voltages. We, therefore, did not control electrode impedances but rather kept direct-current offset close to zero during electrode placement. Vertical and horizontal eye movements were monitored using three additional electrodes placed on the outer canthus of

each eye and on the inferior area of the left orbit. Reference-free electrode signals were amplified, sampled at 2048 Hz (ActiveTwo amplifier, BioSemi, The Netherlands), and stored using BioSemi ActiView Software for offline analysis. Given that auditory stimuli were created online during the experiment, they were recorded using Biosemi' s Analog Input Box (Biosemi, The Netherlands), which was daisy chained by optical fibers to the EEG Analog-to-Digital Converter box and stored alongside the EEG data for future analysis.

Visual Analogue Scales

Participants were given pen and paper analogue scales after each recording block so they could rate their experience after the passive listening task. Two analogue scales were used to determine variations in subjective experience (Rainville et al., 2002). The scales used were:

- Mental relaxation, corresponding to the activity or calmness of the subject' s mind. This dimension spans from a state where the mind is calm, peaceful and in perfect relaxation to a state where the mind is extremely agitated or active.
- Absorption depth corresponds to how the subject feels and how absorbed they felt during the experiment. The scale runs from nonexistent depth to a profound, intense and complete experience.

Data analysis and signal processing

Software Accessibility

All the code used for this project (digital signal processing, data wrangling, and statistics) can be found here: github.com/neurohazardous/binauralBeats.

Visual Analogue Scales

Data from pen and paper scales was measured manually and stored digitally in CSV files for further statistical analysis using R (v3.6.1, R Development Core team, 2008), setting the significance level at 0.05. We first determined the data distribution using a Shapiro-Wilk test. Wherever data was not normal, the specified statistic was compared against a distribution created by permuting the data 1000 times (i.e. scrambling the label of the data), as opposed to comparing the statistic against a parametric distribution (Ernst et al., 2004). We also report confidence intervals obtained from the null distribution (obtained by permuting the data). Given the within-nature of our study, we only performed permutations *within* subjects (e.g. if data was arranged in a matrix were each row is one subject and each column is a measurement, we only permuted the labels of the values within each row). The reported p value was obtained as the number of permuted statistics that were larger than the specified statistic, divided by the total number of

permutations. We analyzed the data using a one-way repeated measures ANOVA for each scale (Mental Relaxation and Absorption Depth) with "Condition" as a 5-level factor (Baseline, Monaural Gamma, Binaural Theta, Binaural Gamma, Monaural Theta). We used *post-hoc* paired t-tests to further disentangle patterns in the data only when the F statistic reached significance. We kept the Family-wise error rate (FWER) at p = 0.05 by using Holm's sequential Bonferroni procedure (see **Table 1**).

EEG

The data was processed using the EEGLAB toolbox (Delorme A. & Makeig S., 2004) and in-house developed scripts in MATLAB. Two different analyses were conducted on the raw EEG data: subcortical (Frequency Following Response) and cortical (Auditory Steady State Response and Functional Connectivity). The pre-processing procedures for either subcortical or cortical analysis differed in filtering process, ICA decomposition and re-referencing. For subcortical analysis, data was high-pass filtered at 100 Hz and re-referenced to linked mastoids. Data used for cortical analysis was bandpass filtered between 1-100 Hz, decomposed using ICA for artifact correction purposes (Jung et al., 1998) and re-referenced to linked mastoids as a first step and then to common average reference as a final step.

Frequency Following Response (FFR)

Data was re-referenced to linked mastoids and high-pass filtered at 100 Hz using a zero-phase Butterworth filter Order 4. Data was visually inspected for noisy electrodes, which were then removed and interpolated using spherical interpolation. Finally, data was epoched into 60 events (from -1 to 7 s with respect to trigger onset) and exported for further analysis. Epochs from each participant were averaged and transformed into the frequency domain using an FFT. From these, power was calculated as the square of the magnitude normalized using a factor of *2/N*, N being the length of the epoch. Frequencies of interest were extracted as the mean of 1 Hz bins around the carrier frequencies (pure tones: 380, 397.5, 403.5, and 420 Hz) for the baseline and each experimental condition. A baseline normalization (decibel change from baseline) was performed to disentangle background dynamics from actual stimulation-related oscillations (Cohen, 2014). The equation used was as follows:

$$dB_f = 10log_{10}\left(\frac{activity_f}{\overline{baseline_f}}\right), \quad \textbf{(1)}$$

where $activity_f$ is a specific frequency power in a given experimental condition and $\overline{baseline_f}$ is the average activity across the whole baseline at a given frequency (Cohen, 2014). The unit of this data is decibel change from baseline.

After baseline normalization, all the scalp channels were averaged together to output one normalized power score per experimental condition per participant. Frequency relevant scores were averaged together in each experimental condition. For example, power scores for 396.5 and 403.5 Hz were averaged together for theta frequency relevant scores. This was done in order to keep the hypothesis testing at a minimum and avoiding inflating the family-wise error rate (FWER). These averaged scores were then exported to R (v3.6.1, R Development Core team, 2008) for hypothesis testing.

We first determined the data distribution using a Shapiro-Wilk test setting the significance level at 0.01. Wherever data was not normal, the specified statistic was compared against a distribution created by permuting the data within each participant for 1000 times (Ernst et al., 2004) and comparing the specified statistic against this distribution. As with the VAS, we report two-tailed confidence intervals (0.95%) obtained from the null distribution. Two sets of data were analyzed (power at relevant gamma and relevant theta frequencies) with 64 scores each (4 conditions x 16 participants) for statistical significance. A factorial (2x2) repeated measures ANOVA was computed per relevant pure tone data set (Theta and Gamma) using beat type (binaural, monaural) and frequency (gamma, theta) as within factors. When the interaction between the factors was significant, we calculated post-hoc paired t-tests to further disentangle

296 patterns in the data (i.e., identify which experimental condition elicited the highest response). We
297 used Holm' s sequential Bonferroni correction to keep the FWER at 0.05 (see **Table 1)**.
298

299 Auditory Steady State Responses (ASSR)

300 Data was imported and re-referenced to linked mastoids. Data was then resampled at 512 Hz,
301 trimmed around the time-window of interest (8m ± 3s) and filtered twice: using a 2nd order
302 Butterworth band-pass filter (zero-phase) between 1-100 Hz, and an FIR notch filter at 60 Hz
303 (minimizing line noise). Data was visually inspected for noisy electrodes, which were then
304 removed.

305 For each participant, ICA decomposition was applied to the full recording of all conditions.
306 Prior to this, these aggregated files were first filtered between 1 and 80 Hz and decimated to 256
307 Hz. Data was then decomposed using the *runica()* function from EEGlab (which uses the Bell &
308 Sejnowski' s (1995) ICA algorithm and Lee, Girolami & Sejnowski' s extended-ICA algorithm
309 (2000)). After visual inspection of individual components, weight matrices were obtained from this
310 decomposition and applied to the original five files for artifact correction purposes (remove
311 components deemed as non-cortical activity, Jung et al., 1998). Missing electrodes were
312 interpolated after ICA artifact correction. EEG was re-referenced to common average (CAR) and

epoched from -1s to 8s relative to trigger onset. Finally, data was baseline corrected (using whole epoch as the baseline) and stored for further analysis.

Each participant' s epochs were averaged and transformed into the frequency domain using an FFT. From these, power was calculated as the square of the magnitude normalized using a factor equal to $2/N$, where N is the number of samples in each sequence. Frequencies of interest were extracted as the mean of 1 Hz bins around beat frequencies (7 and 40 Hz) for both the baseline and each experimental condition. As with the FFR preprocessing procedure, a baseline normalization (decibel change from baseline) was done using **Equation 1**.

After baseline normalization, all channels were averaged together to output one normalized power score per experimental condition per participant. These scores were then exported to R (v3.6.1, R Development Core team, 2008) for hypothesis testing.

Statistical analyses were very similar to those done for the FFR analysis. We first determined the data distribution using a Shapiro-Wilk test. Wherever data was not normal, the specified statistic was compared against a distribution created by permuting the data within each participant for 1000 times (Ernst et al., 2004) and comparing the specified statistic against this distribution. We report two-tailed confidence intervals (0.95%) obtained from this null distribution. Two statistical analysis were performed: one on normalized power scores at gamma beat frequency and one on normalized power scores at theta beat frequency (each had 64 scores

total, 4 conditions x 16 participants). Hypothesis testing was performed using a factorial (2x2) repeated measures ANOVA with beat type (binaural, monaural) and frequency (gamma, theta) as within factors. Finally, *post-hoc* paired t-tests were calculated wherever there was a significant interaction between factors to identify which experimental conditions elicited the highest entrainment. We used Holm' s sequential Bonferroni procedure to keep the Family-wise error rate (FWER) at 0.05 (see **Table 1**).

Functional Connectivity

Two complementary measurements of Functional Connectivity were used as indices of long-range synchronization: Phase locking value (PLV; Lachaux et al., 2000)) and Imaginary Coherence (iCOH; Nolte et al., 2004). On top of that, per electrode, the amplitude of the Hilbert Transform and the Power of the Fourier transform were computed as local indices of synchronization. Analyses were done over all traditional frequency bands (Delta: 1 - 4 Hz; Theta: 5 - 8 Hz, Alpha: 9 - 12 Hz, Beta: 13 - 30 Hz, Gamma: 32 - 48 Hz) and the specific beat frequencies (1Hz bins around 7Hz and 40 Hz). ICA corrected data (i.e. the same files used for ASSR) was imported to MATLAB to compute these metrics.

348 Hilbert Transform and PLV

349 The phase locking value (PLV) looks at how stable phase differences are between signals (in this
350 case, electrodes). In this particular implementation, it determines, on average, how stable phase
351 differences between electrodes are within trials (i.e., over time). PLV is only sensitive to phase
352 differences between signals (not their amplitude) at the cost of not being able to distinguish
353 spurious correlation due to volume conduction at the scalp level from actual connectivity between
354 two cortical regions (Lachaux et al., 1999).

355 To calculate it, the signal of interest was extracted by band-passing the ICA corrected data
356 using a finite impulse response filter (FIR) around both the traditional frequency bands of interest
357 and the specific beat frequencies: Delta (1 - 4 Hz), Theta (5 - 8 Hz), Alpha (9 - 12 Hz), Beta (13 - 30
358 Hz), Gamma (32 - 48 Hz), Theta Beat (6 - 8 Hz) and Gamma Beat (39 - 41 Hz). Phase and
359 amplitude of the analytical signal (Hilbert transform) were then extracted for each EEG channel.
360 For each pair of electrodes, the PLV was computed as a long-distance synchronization index on
361 eight-second non-overlapping sliding windows as

362

363 $$PLV_{i,j} = \left|\frac{1}{N}\sum_{t=1}^{N} e^{i(\phi_i(t)-\phi_j(t))}\right|, \quad \textbf{(2)}$$

364

where N is the number of samples considered in each eight second window, ϕ is the phase and $||$ the complex modulus. Thus, PLV measure equates 1 if the two signals are perfectly phase locked across the whole observed time window and equates 0 if they are totally unsynchronized. For each electrode, the amplitude of the analytic signal (Hilbert Transform) was stored as a local synchronization index. Nonparametric permutation testing was used to gauge the statistical significance of the effects of binaural and monaural beats on Functional Connectivity.

Fourier Transform and iCOH

Coherency (Magnitude-Squared Coherence) between two EEG channels can be defined as the measure of a linear relationship (i.e. correlation) between two signals (in this case, electrodes) at specific frequencies. It is calculated as the cross-spectral density between channels *i* and *j*, normalized by the square root of the multiplication of each of their own auto-spectrums. By projecting the results into the imaginary axis, we rid the signal of both immediate (a phase difference of 0) and anti-phase (phase difference of π) connectivity patterns. The imaginary part of coherence is insensitive to spurious correlations due to volume conduction at the expense of being sensitive to signals' amplitude (as well as phase) and being unable to disentangle spurious from real immediate connectivity patterns (both in phase and anti-phase; Nolte et al. 2004).

Imaginary coherence measures were extracted on eight-second non-overlapping sliding windows (similar to the PLV procedure):

$$iCOH_{i,j} = \sum_{f=f1}^{f2} Im\left(\frac{S_{i,j}(f)}{\left(S_{i,i}(f)S_{j,j}(f)\right)^{1/2}}\right) \text{ with } S_{i,j}(f) =< x_i(f)x_j^*(f) >, \quad \textbf{(3)}$$

where $x_i(f)$ and $x_j(f)$ are the complex Fourier transforms of channels *i* and *j* respectively, * stands for complex conjugation, <> for the expectation value, f_1 and f_2 are the boundary of the considered frequency band, $S_{i,j}(f)$ is the cross-spectral density between channels *i* and *j*, and $Im()$ is the imaginary part of a complex number. As a long-distance synchronization index, iCOH values were averaged for each pair of electrodes across frequency bins using a tolerance of 1 Hz (e.g., 7 ± 1 Hz). Each electrode' s autospectrum was stored as a local synchronization index. As with PLV and Hilbert Transform, nonparametric permutation testing was used to gauge the statistical significance of the effects of binaural and monaural beats on Functional Connectivity.

Cross-frequency interactions

In this context, we consider cross-frequency interactions as activity elicited by either experimental condition (binaural or monaural) that is outside of the frequency range of the beat (either 7 Hz for

theta, or 40 Hz for gamma). For example, activity in the alpha frequency band elicited by theta experimental conditions is considered as a cross-frequency interaction (Solcà et al., 2016).

Neurophenomenological analysis

To explore the relationship between mood (as self-reported by the visual analogue scales) and neural patterns of Functional Connectivity, each participant' s two highest rated experimental conditions (binaural gamma, monaural theta…) were contrasted with the two lowest rated ones for each visual analogue scale. These contrasts were then averaged across participants for each scale (Mental Relaxation and Absorption Depth). Again, non-parametric permutation testing was used to gauge the statistical significance of the relations between subjective experience and Functional Connectivity.

Functional Connectivity: Nonparametric statistics

Given the exploratory nature of our study, we decided to use nonparametric permutation testing to maintain the family-wise error rate (FWER) at 5%, as it offers a straightforward solution to the multiple-comparisons problem (see Maris & Oostenveld, 2007 and Groppe et al., 2011). The critical *t* value was determined for all Functional Connectivity analysis (PLV, iCOH, autospectrum,

Hilbert transform, and neurophenomenology) as follows: (1) the experimental conditions were contrasted with each other (binaural vs. monaural control) and each experimental condition was contrasted with baseline, (2) a *t*-test was performed at each spatial-spectral point (i.e. electrode at a given frequency), (3) the statistics were normalized using z-scores, (4) the cluster statistic was considered to be the sum of all *t*-values of the cluster members exceeding 3 in absolute value, (5) 1,000 permutations of the data were then performed to obtain a distribution of cluster statistics under the null hypothesis and determine the critical values. All randomizations were done for a rejection of the null hypothesis and a control of false alarm rate at $p < 0.05$. We decided to choose this method to correct for multiple comparisons because we are mainly interested in broadly distributed effects (Groppe et al., 2011). To make our inferences more conservative, only contrasts that exhibit at least three significant spatio-spectral points are shown here (i.e., electrodes at a given frequency).

Results

Frequency Following Response (FFR)

To keep analyses consistent, we performed permutation-based statistics when testing for the FFR' s significance.

Theta Pure Tones (396.5 & 403.5 Hz)

Both theta binaural and monaural beats elicited an FFR at theta carrier frequencies with no difference between them (average of 396.5 Hz and 403.5 Hz; **Figure 3a**). There was a main effect of beat frequency ($F=34.57$, $p=0.001$)[c], with no effect of beat type ($F=0.004$, $p=0.96$)[c] nor an interaction between the factors ($F=1.169$, $p=.292$)[c].

Gamma Pure Tones (380 & 420 Hz)

Gamma binaural and monaural beats elicited an FFR at gamma carrier frequencies (average of 380 Hz and 420 Hz; **Figure 3b**), with no difference between them. There was a main effect of

frequency (F=26.648, p=0.001)[d] with no effect of beat type (F=0.057, p=0.828)[d] nor an interaction between the factors (F=1.248, p=0.271)[d].

Auditory Steady State Response (ASSR)

To keep analyses consistent, we performed permutation-based statistics when testing for the ASSR' s significance.

Theta ASSR (7 Hz)

Theta binaural and monaural conditions elicited an ASSR at beat frequency, with monaural beats peaking higher than binaural beats (**Figure 4a**). There was both a main effect of beat type (F=7.669, p=0.018)[e] and beat frequency (F=19.263, p=0.001)[e], with no interaction (F=3.928, p=0.075)[e].

Gamma ASSR (40 Hz)

Gamma beats (both binaural and monaural) elicited an ASSR at 40 Hz, with binaural gamma eliciting the highest power (**Figure 4b**). There were main effects of both beat type (F=34.538,

p=0.001)[f] and beat frequency (F=51.933, p=0.001)[f], as well as an interaction between the two factors (F=44.284, p=0.001)[f]. To further disentangle these differences, three post-hoc pairwise comparisons were done using Holm' s sequential Bonferroni correction test. The first two comparisons confirmed that monaural gamma peaked the highest at 40 Hz when compared to both binaural gamma (Mean difference=6.2702, t=7.23 p_{corr}=0.002)[f] and monaural theta (Mean Difference=7.6589, t=7.68 p_{corr}=0.003)[f]. Binaural gamma condition elicited a stronger ASSR than binaural theta at 40 Hz (Mean Difference=1.1888, t=2.46, p_{corr}=0.025)[f].

Functional Connectivity

Phase-locking value (PLV) and Hilbert Transform Amplitude

Both binaural and control conditions elicited within and cross-frequency patterns at long and short ranges. These were dependent on both beat type and frequency. In terms of local synchronization (Hilbert Transform Amplitude), Monaural Gamma stimulation drove a positive frontoparietal cluster at 40 Hz (gamma beat) when contrasted with baseline (**Figure 5a**, CS=20.52, p=0.019)[g]. In terms of long-distance synchronization (PLV), we found a positive left-occipital to frontoparietal cluster of activity at 40 Hz (Figure 4b, CS=49.827, p=0.041)[h] when contrasting binaural theta with monaural theta experimental conditions. When contrasting binaural gamma

with monaural gamma, we found four clusters of activity: a positive cluster extending around the scalp at alpha frequency band (**Figure 5c top left**, CS=1043.455, p=0.002)[h], a negative central-occipital cluster at gamma frequency band (**Figure 5c top right**, CS=-219.57, p=0.043)[h]; a negative frontal cluster at gamma frequency band (**Figure 5c center**, CS=-240.17, p=0.028)[h]; and a negative scalp-wise cluster at 40 Hz (**Figure 5c bottom left**, CS=-2695.07, p=0.002)[g]. Consistent with the last cluster, the monaural gamma condition drove a positive scalp-wise cluster when contrasted with baseline (**Figure 5c bottom right**, CS=2493.34, p=0.004)[h].

Imaginary Coherence (iCOH) and Fourier Transform Power

As indexed by iCOH and Fourier Transform, we only found short distance synchronization elicited by binaural theta conditions. In terms of local synchronization (Fourier Power), we found two clusters of activity when contrasting binaural theta condition with baseline: a negative central-parietal cluster of activity at theta frequency band (**Figure 6, top**; CS=-11.45, p=0.036)[i] and a positive left central-temporal cluster at 40 Hz (**Figure 6 bottom**; CS=36.10, p=0.018)[i]. None of the other contrasts reached our criteria for significance ($p < 0.05$ and a cluster of at least three sensors).

Neurophenomenological analysis

When taking into consideration individual differences due to subjective experience, we find neural connectivity patterns associated with high Absorption Depth and Mental Relaxation that are consistent across participants. When contrasting each participants' two highest and two lowest rated experimental conditions in terms of mental relaxation, we found one negative frontal cluster of local activity (**Hilbert Transform, Figure 7a**) at Theta frequency band (CS=-9.51, p=0.026)[j], and a negative long-range frontocentral to occipital cluster of activity (**iCOH**) at the same frequency band (**Figure 7c left** iCOH: CS=-61.95, p=0.034)[j]. We also found a frontal to right-temporal-occipital negative cluster of activity at 40 Hz (**Figure 7c right** iCOH: CS=-97.33, p=0.043)[j]. On the other hand, we also contrasted the two top experimental conditions in which a given participant rated absorption depth the highest with the experimental conditions in which they rated absorption depth the lowest. We found a right temporal negative cluster of local (Fourier Power) activity at 40 Hz (**Figure 7b**; CS=-10.17, p=0.05)[j].

Visual Analogue Scales

There was no effect from auditory stimulation on subjective ratings (**Figure 2**). To keep analyses consistent throughout the manuscript, we performed permutation-based statistics. There were no

differences between the five levels of the factor Condition (baseline, binaural gamma, binaural theta, monaural gamma, monaural theta) neither in Mental Relaxation ($F=1.698$, $p=0.158$)[a] nor Absorption Depth ($F=1.313$, $p= 0.291$)[b]. These suggest that subjective experience related to each experimental condition was not different from baseline nor from each other.

Discussion

Here, we asked whether binaural beats are able to elicit neural entrainment, and modulate mood, in a specific fashion compared to a control rhythmic stimulus. To do so, we used a passive, single-blind listening task where participants were exposed to both binaural and monaural control conditions while we recorded their electrical brain activity and mood self-reports. By comparing activity between binaural and monaural control conditions at different levels (subcortical, cortical and self-reports), we found that binaural beats did entrain the brain, but the control condition did so more strongly, with none of them showing an effect on mood. Furthermore, while distinct Functional Connectivity patterns emerged for both binaural and monaural beats at different frequencies, these are not consistent with previous literature and are not related to participants' self-reported mood.

Binaural and monaural beats elicit subcortical responses at carrier frequencies

Though it is commonly agreed that Binaural Beats originate in the brainstem (Oster, 1973; Moore, 2012; Wernick & Starr, 1968), to the best of our knowledge, we are the first ones to investigate this particular stimulus at subcortical levels using EEG. As we predicted, both experimental conditions (theta and gamma), regardless of beat type, elicited a frequency following response at the pure tone frequencies, with no difference between monaural and binaural beats. This is consistent with the existing auditory brainstem response literature, where the generated subcortical responses are found to have a close spectrotemporal structure to the patterns of an acoustic stimulus, such as speech syllables (Skoe & Kraus, 2010; Lehmann & Schönwiesner, 2014). Furthermore, given our choice of carrier frequencies (around 400 Hz), it is very unlikely these responses have a cortical origin (Coffey et al., 2016). The lack of difference between beat types suggests that both stimuli are processed in a similar way at the subcortical level.

Monaural beats elicit higher cortical entrainment at the beat frequency than their binaural counterparts

Both beat types entrained the brain at their beat frequencies, with monaural conditions eliciting the highest response when compared to binaural conditions. In terms of Theta beat frequency, both Jirakittayakorn & Wongsawat (2017) and Karino et al. (2006), found similar entrainment using Theta binaural beats with exposure times between five and ten minutes. Following Garcia-Argibay' s conclusions (2018), relatively long exposure time and non-masked binaural beats (i.e., not using white or pink noise to mask them) seem to optimize the responses to the beats. In terms of Gamma beat frequency, we successfully replicated previous studies (Schwarz & Taylor, 2005; Draganova et al., 2007; Ross et al., 2014): both binaural and monaural gamma beats entrain cortical activity at 40Hz, but binaural beats elicit less power at the beat frequency. One possible explanation as to why binaural beats elicit less power than monaural beats is that the entrainment we measure at the cortical level might be caused by the perceived rhythmicity, and not the binaural beat itself. Subjects' tended to report that the modulation (i.e., the beat) intensity in binaural beats was weaker than that of the monaural beat. The ASSR correlates with stimulus' loudness (Van Eeckhoutteet al., 2016; Picton et al., 2007; Lins & Picton, 1995), which might explain the difference in ASSR power in the frequency domain. Furthermore, we both root mean squared

(rms) normalized and carefully calibrated our stimuli, precluding loudness as an explanatory factor for the difference in ASSR power. Using proper statistical and experimental control, we have shown that binaural beats entrain the cortex more weakly than other non-binaural rhythmic stimuli, such as monaural beats.

Binaural and monaural beats fail to modulate mood

Echoing previous reports, we did not find evidence of binaural beats, nor monaural beats, modulating cognitive states or mood: López-Caballero & Escera (2017) found no emotional regulation due to binaural beats as indexed by changes in heart rate and skin conductance, while Gálvez et al. (2018) found no modulation of anxiety as indexed by the State Anxiety Inventory (SAI). This stands in contrast with other reports where cognitive performance and mood were successfully modulated by binaural beats (Wahbeh et al., 2007, Le Scouarnec et al., 2001, Padmanabhan et al., 2005; Isik et al., 2017, Reedijk et al., 2013; Reedijk et al., 2015, Garcia-Argibay et al., 2018).

Both beat types elicit differential short-range connectivity patterns

Monaural and binaural beats affect short range electrode level connectivity patterns differentially. We only found a significant short-range effect in monaural gamma and binaural theta conditions, which suggests that both beat type and frequency are non-trivial parameters of stimulation. Furthermore, due to both binaural and monaural beats producing such short-range effect, we can rule out conclusions such as this activity being a by-product of sustained listening or binaural integration. Our gamma findings are in accordance with those from Becher et al. (2015). Using both intracranial and scalp EEG, they found peak EEG power at 40 Hz (gamma beat) at the scalp electrodes using the power of the envelope of the signal (i.e., the power of the Hilbert Transform). They found a similar effect in temporo-lateral intracranial electrodes, suggesting this entrainment originates in auditory cortices. Furthermore, they found a significant decrease in EEG power at 5 Hz (theta frequency) in temporo-basal anterior and posterior areas, which might explain the local activity in our participants. This activity could be in line with a dipole from auditory cortices pointing upwards, which suggests there is only one active cortical source. On the other hand, binaural theta conditions elicited a positive parietal cluster at 40 Hz (see cross

frequency section). The functional meaning (if any) of these short-range patterns remains unclear as we found no difference in participants' self-reports.

Both beats elicit long-range connectivity patterns indexed only by PLV

To investigate long-range connectivity, we used two different but complementary statistics: the imaginary part of coherence and the phase locking value. iCOH gets rid of all interactions that have zero to very small time delays, while the PLV quantifies how consistent phase differences are between electrodes. We only found Functional Connectivity patterns indexed by PLV. Because of this, it is unclear whether these patterns are due to one source being propagated around the scalp, or there are multiple sources active with an almost zero-time delay between them (Nolte et al., 2004). We see differential effects between beat types and frequencies, as well as cross-frequency interactions (discussed in the next section). Only gamma experimental conditions elicited within frequency activity: Monaural gamma elicited a cluster of scalp-wise connectivity that is not consistent with previous research. Using intracranial electrodes, Becher et al. (2015) showed phase desynchronization at mediotemporal areas using a 40 Hz monaural beat, whereas

we found scalp-wise synchronization using a very similar stimulus. Furthermore, Schwarz & Taylor (2005) showed that there was a delay of several milliseconds in the activity elicited across the fronto-occipital axis, using a 40 Hz monaural beat, suggesting multiple cortical sources of activity. Because the iCOH analysis did not reveal significant connections between electrodes, it is unclear whether the phase differences Schwarz & Taylor (2005) report are due to volume conduction or the connectivity patterns we found are caused by multiple, but tightly synchronized, brain regions. Because we did not find any difference in subjective reports, the functional meaning (if any) of this activity remains unclear.

Binaural beats elicit cross-frequency connectivity patterns

Binaural theta conditions elicit a front to back, cross-frequency connectivity pattern at gamma beat frequency (40 Hz) while binaural gamma elicits a widespread connectivity pattern at alpha frequency. In line with our results, several groups have found binaural beats eliciting activity outside of the frequency range of the beat. Despite this, these findings do not seem to be consistent: using theta binaural beats, Gao et al. (2014) found a decrease in relative beta power

over left temporal areas and Ioannou et al. (2015) report no significant difference from theta binaural beats at other frequency bands.

We found that binaural theta beats elicit activity at higher frequencies (40 Hz), while binaural gamma beats elicit activity at lower frequencies. This cross-frequency coupling (low frequency driving a higher frequency and a higher frequency driving a lower frequency) could be evidence for large-scale integration being enhanced by binaural beats. Varela et al. (2001) argue that slower rhythms (such as theta) provide a temporal framing for faster oscillations. For example, gamma oscillations are thought to leverage this slower temporal framing during successive cognitive moments of synchronous assemblies where memory is consolidated (Osipova et al., 2006; Burke et al., 2013; Lisman & Jensen, 2013). We did not investigate cognitive processes directly, but there is evidence that binaural beats impact memory as a function of beat frequency—beta frequencies seems to enhance it (Lane et al., 1998; Kennerly et al., 1994; Beauchene et al., 2016; Gálvez et al., 2018) while theta frequencies have an inconsistent effect (negative in some cases: Garcia-Argibay et al., 2017, Beauchene et al., 2016; and positive in others: Ortiz et al., 2008). In our specific experiment, our stimuli failed to modulate mood as self-reported by participants, but these cross-frequency interactions might provide a framework explaining why binaural beats are able to modulate cognitive performance in other reports.

Individual differences shed light on connectivity patterns associated with specific cognitive states

We found a consistent pattern of deactivation and desynchronization related to participants' self-reports of Mental Relaxation and Absorption Depth. High Mental Relaxation was associated with theta frequencies in a frontal cluster of local desynchronized activity, and with a front to back desynchronization of activity at both theta and gamma indexed by iCOH. This suggests this activity is robust and not due to volume conduction. Absorption Depth, on the other hand, was associated with one cluster of activity around temporal areas. Changes in the anterior and frontal midline in theta power have been related to emotionally positive states (Aftanas & Golocheikine, 2001), and meditation-related states (Baijal & Srinivasan, 2010). Baijal & Srinivasan (2010) found a similar deactivation pattern in parietal and occipital areas accompanied by frontal theta activation associated with meditative states. On the other hand, Hinterberger et al. (2014) found similar central and parietal gamma deactivation patterns during meditative tasks. Taking all this information together, our Functional Connectivity results point at a state similar to meditation characterized by heightened Mental Relaxation and Absorption Depth. Despite this, we were not able to relate this specifically to any of our experimental conditions.

Limitations and Future Directions

Though several of our findings are consistent with existing literature, we acknowledge that we only recruited 16 people and that these findings should be replicated with higher sample sizes. We instructed participants to close their eyes during the whole experiment, which might have not been ideal, especially because a couple of participants reported high drowsiness and two reported falling asleep. Furthermore, we did not have a specialist check our participants for any hearing loss. This could be a co-founding variable. Our design, however, was a within design: each participant was exposed to the four experimental conditions. Because participants were only compared against themselves (statistically speaking), this co-founding effect remained constant for each participant. Future binaural beats studies should look at different ways of indexing connectivity at both scalp and source level (Solcà et al, 2016). The study of binaural beats will also greatly benefit from the transition of a mass univariate statistical framework (such as the one used here) to a multivariate statistical framework (see McIntosh & Mišić, 2013). Fields such as Graph Theory present promising opportunities to determine the characteristics of cortical networks and summarizing large numbers of data points into a few statistics to truly understand how binaural beats affect the brain (Ioannou et al., 2015; Ala et al., 2018). On a more technical note, we did not alternate the polarity of the stimulus of the binaural beats (a common practice in the Auditory

673 Brainstem Response literature), which might have affected the brainstem responses we found.
674 Sometimes, noise from the audio transducer or the cochlear microphonic (a potential believed to
675 be generated primarily by outer hair cells; Santarelli et al., 2006) can bleed into the EEG electrodes,
676 introducing artifactual responses into the EEG trace. To minimize this, one can alternate the
677 polarity of the stimulus between each presentation, i.e., by presenting the original stimulus
678 followed by a version of the stimulus that has been multiplied by minus one and repeating this
679 over and over. After this, the EEG responses to both polarities can be either added or subtracted
680 together (each method has its advantages and disadvantages). For an in-depth discussion of this,
681 see Skoe & Kraus, 2010. The transducer with which the stimuli were presented to the participants
682 was magnetically shielded, a procedure that is known to minimize stimulus artifacts (Skoe &
683 Kraus, 2010). Furthermore, Skoe & Kraus (2010) report that '[their] results have been internally
684 replicated with single-polarity stimuli', supporting our claim that the responses we report here
685 come from the brainstem and are not artifactual.

686 Binaural beats have been long used in psychoacoustics, although the claims and studies
687 relating their cognitive effects are more recent. A great deal of confusion subsides regarding their
688 latter use. As Garcia-Argibay et al. (2018) concluded, there are several mediating variables—such
689 as beat frequency, exposure time or stimulus masking—that are not always clearly reported.
690 Furthermore, we conclude that there are two important factors that are usually considered as

trivial: proper EEG analysis and the use of a proper control condition. Future binaural beats studies should be mindful of these variables and report them accordingly. Several studies that did not find any entrainment to the beat frequency of binaural beats (e.g., López-Caballero & Escera, 2017) did not use standard normalization practices (for an in-depth discussion of these procedures, see Cohen, 2014, Ch. 18). The human EEG spectrum exhibits a 1/f power scaling (similar to pink noise). By properly normalizing data using a baseline condition, we ensure that all data (i.e. the different frequency bands) will have the same scale, and we are appropriately disentangling background and task-unrelated dynamics (Cohen, 2014). Researchers should be mindful of the analysis approach they are taking, as well as using an appropriate control condition to truly elucidate whether binaural beats are a special kind of stimulus or their advantages are due to stimulus properties (such as the rhythmicity in the signal).

Future studies should carefully choose exposure time, the performance or mood measurement and the frequency of the beat. As Garcia-Argibay et al. (2018) concluded, higher exposure times are associated with larger effect sizes. Nevertheless, whether several sessions will present an increased entrainment and performance/mood boost, and whether there are carryover effects that are sustained even after stimulation ceases, are still open questions. Binaural beats have previously been reported to modulate memory and attention performance (Ortiz et al., 2008; Reedijk et al., 2015), as well as anxiety (Isik et al., 2017) and analgesia (Zampi, 2015). Our findings

provide one plausible base explanation as to why memory and attention performance could be modulated by binaural beats (i.e. binaural beats elicit cross-frequency interactions). Future studies should focus on measuring cognitive performance on both attention and memory tasks, and mood regulation related to anxiety and pain perception. Participants should be exposed to the stimulation both before and after the task (Garcia-Argibay et al., 2018). Finding neural correlates of binaural beats that uniquely correlate with cognitive performance in attention and memory tasks could help better elucidate whether binaural beats can be used for cost-effective cognitive enhancement. Finally, the choice of frequency is not trivial: alpha, beta, and gamma were reported to provide positive effects in memory tasks, while theta frequency seems to hinder effects in most cases (Garcia-Argibay et al., 2018).

Conclusions

Using a factorial experimental design and a single-blind, passive listening task, we aimed to elucidate the impact of binaural beats on the brain. We did not find evidence for binaural beats modulating mood or entraining the brain more strongly than "non-binaural" beats. We did find, however, that binaural beats elicited differential patterns of connectivity, compared to the monaural beat control. Whether these connectivity patterns have a functional meaning (in terms

of cognitive enhancement and mood modulation) remains an open question. The present research shares a useful framework for further exploring the mechanisms and efficacy of sound-based mood regulation practices. By using a neuroscientific lens with statistical and scientific rigor at its core, we can study these "alternative" practices to ensure the general public makes informed, evidence-based, decisions.

References

Aftanas, L. I., & Golocheikine, S. A. (2001). Human anterior and frontal midline theta and lower alpha reflect emotionally positive state and internalized attention: high-resolution EEG investigation of meditation. *Neuroscience Letters*, 310(1), 57-60.

Ala, T. S., Ahmadi-Pajouh, M. A., & Nasrabadi, A. M. (2018). Cumulative effects of theta binaural beats on brain power and Functional Connectivity. *Biomedical Signal Processing and Control*, 42, 242-252.

Atwater, F. H. (1997). Accessing anomalous states of consciousness with a binaural beat technology. *Journal of Scientific Exploration*, 11(3), 263-274.

Atwater, F. H. (2004). The hemi-sync process. *The Monroe Institute*, VA.

742 Baijal, S., & Srinivasan, N. (2010). Theta activity and meditative states: spectral changes during
743 concentrative meditation. *Cognitive Processing*, 11(1), 31-38.
744 Becher, A.-K., Höhne, M., Axmacher, N., Chaieb, L., Elger, C. E., & Fell, J. (2015). Intracranial
745 electroencephalography power and phase synchronization changes during monaural and
746 binaural beat stimulation. *European Journal of Neuroscience*, *41*(2), 254–263.
747 https://doi.org/10.1111/ejn.12760
748 Beauchene, C., Abaid, N., Moran, R., Diana, R. A., & Leonessa, A. (2016). The effect of binaural
749 beats on visuospatial working memory and cortical connectivity. *PLOS ONE*, 11(11),
750 e0166630.ç
751 Bell, A. J., & Sejnowski, T. J. (1995). An information-maximization approach to blind separation and
752 blind deconvolution. *Neural Computation*, 7(6), 1129-1159.
753 Bernardi, L., Sleight, P., Bandinelli, G., Cencetti, S., Fattorini, L., Wdowczyc-Szulc, J., & Lagi, A.
754 (2001). Effect of rosary prayer and yoga mantras on autonomic cardiovascular rhythms:
755 comparative study. Bmj, 323(7327), 1446-1449.
756 Bernardi, N. F., Snow, S., Peretz, I., Perez, H. O., Sabet-Kassouf, N., & Lehmann, A. (2017).
757 Cardiorespiratory optimization during improvised singing and toning. Scientific reports,
758 7(1), 8113.

759 Burke, J. F., Zaghloul, K. A., Jacobs, J., Williams, R. B., Sperling, M. R., Sharan, A. D., & Kahana, M. J.
760 (2013). Synchronous and asynchronous theta and gamma activity during episodic memory
761 formation. *Journal of Neuroscience*, 33(1), 292-304.
762 Canolty, R. T., & Knight, R. T. (2010). The functional role of cross-frequency coupling. Trends in
763 cognitive sciences, 14(11), 506-515.
764 Chaieb, L., Wilpert, E. C., Reber, T. P., & Fell, J. (2015). Auditory Beat Stimulation and its Effects on
765 Cognition and Mood States. *Frontiers in Psychiatry*, *6*.
766 https://doi.org/10.3389/fpsyt.2015.00070
767 Coffey, E. B., Herholz, S. C., Chepesiuk, A. M., Baillet, S., & Zatorre, R. J. (2016). Cortical
768 contributions to the auditory frequency-following response revealed by MEG. *Nature*
769 *Communications*, 7, 11070.
770 Cohen, M. X. (2014). Analyzing neural time series data: theory and practice. *MIT Press*.
771 Colzato, L. S., Barone, H., Sellaro, R., & Hommel, B. (2017). More attentional focusing through
772 binaural beats: evidence from the global–local task. *Psychological Research*, *81*(1), 271–277.
773 https://doi.org/10.1007/s00426-015-0727-0
774 Colzato, L. S., Steenbergen, L., & Sellaro, R. (2017). The effect of gamma-enhancing binaural beats
775 on the control of feature bindings. *Experimental Brain Research*, *235*(7), 2125–2131.
776 https://doi.org/10.1007/s00221-017-4957-9

777 Delorme A & Makeig S (2004) EEGLAB: an open source toolbox for analysis of single-trial EEG
778 dynamics. *Journal of Neuroscience Methods*. 134:9-21
779 Draganova, R., Ross, B., Wollbrink, A., & Pantev, C. (2007). Cortical steady-state responses to
780 central and peripheral auditory beats. *Cerebral Cortex*, 18(5), 1193-1200.
781 Ernst, M. D. et al. (2004). Permutation methods: a basis for exact inference. Statistical Science
782 19(4), 676–685.
783 Gao, X., Cao, H., Ming, D., Qi, H., Wang, X., Wang, X., … Zhou, P. (2014). Analysis of EEG activity in
784 response to binaural beats with different frequencies. *International Journal of*
785 *Psychophysiology*, *94*(3), 399–406. https://doi.org/10.1016/j.ijpsycho.2014.10.010
786 Gálvez, G., Recuero, M., Canuet, L., & Del-Pozo, F. (2018). Short-Term Effects of Binaural Beats on
787 EEG Power, Functional Connectivity, Cognition, Gait and Anxiety in Parkinson' s Disease.
788 *International Journal of Neural Systems*, 28(05), 1750055.
789 Garcia-Argibay, M., Santed, M. A., & Reales, J. M. (2017). Binaural auditory beats affect long-term
790 memory. *Psychological Research*. https://doi.org/10.1007/s00426-017-0959-2
791 Garcia-Argibay, M., Santed, M. A., & Reales, J. M. (2018). Efficacy of binaural auditory beats in
792 cognition, anxiety, and pain perception: a meta-analysis. *Psychological Research*, 1-16.
793 Groppe, D. M., Urbach, T. P., & Kutas, M. (2011). Mass univariate analysis of event-related brain
794 potentials/fields I: A critical tutorial review. *Psychophysiology*, 48(12), 1711-1725.

795 Hillebrand, A., Barnes, G. R., Bosboom, J. L., Berendse, H. W., & Stam, C. J. (2012). Frequency-
796 dependent Functional Connectivity within resting-state networks: An atlas-based MEG
797 beamformer solution. *NeuroImage*, 59(4), 3909–3921.
798 https://doi.org/10.1016/j.neuroimage.2011.11.005
799 Hinterberger, T., Schmidt, S., Kamei, T., & Walach, H. (2014). Decreased electrophysiological
800 activity represents the conscious state of emptiness in meditation. *Frontiers in Psychology*,
801 5, 99.
802 Ioannou, C. I., Pereda, E., Lindsen, J. P., & Bhattacharya, J. (2015). Electrical Brain Responses to an
803 Auditory Illusion and the Impact of Musical Expertise. *PLOS ONE*, *10*(6), e0129486.
804 https://doi.org/10.1371/journal.pone.0129486
805 Isik, B. K., Esen, A., Büyükerkmen, B., Kilinç, A., & Menziletoglu, D. (2017). Effectiveness of binaural
806 beats in reducing preoperative dental anxiety. *British Journal of Oral and Maxillofacial*
807 *Surgery*, *55*(6), 571–574. https://doi.org/10.1016/j.bjoms.2017.02.014
808 Jirakittayakorn, N., & Wongsawat, Y. (2017). Brain responses to a 6-Hz binaural beat: Effects on
809 general theta rhythm and frontal midline theta activity. *Frontiers in Neuroscience*, 11, 365.
810 Jung, T.-P., Humphries, C., Lee, T.-W., Makeig, S., McKeown, M. J., Iragui, V., … others. (1998).
811 Extended ICA removes artifacts from electroencephalographic recordings. *Advances in*
812 *Neural Information Processing Systems*, 894–900.

Karino, S., Yumoto, M., Itoh, K., Uno, A., Yamakawa, K., Sekimoto, S., & Kaga, K. (2006). Neuromagnetic responses to binaural beat in human cerebral cortex. Journal of neurophysiology, 96(4), 1927-1938.

Kennerly, R. C. (1994). An empirical investigation into the effect of beta frequency binaural beat audio signals on four measures of human memory (Master's thesis, West Georgia College).

Kuwada, S., Yin, T. C., & Wickesberg, R. E. (1979). Response of cat inferior colliculus neurons to binaural beat stimuli: possible mechanisms for sound localization. *Science*, 206(4418), 586-588.

Lachaux, J. P., Rodriguez, E., Le Van Quyen, M., Lutz, A., Martinerie, J., & Varela, F. J. (2000). Studying single-trials of phase synchronous activity in the brain. *International Journal of Bifurcation and Chaos*, 10(10), 2429-2439.

Lagopoulos, J., Xu, J., Rasmussen, I., Vik, A., Malhi, G. S., Eliassen, C. F., ... Holen, A. (2009). Increased theta and alpha EEG activity during nondirective meditation. *The Journal of Alternative and Complementary Medicine*, 15(11), 1187–1192.

Lane, J. D., Kasian, S. J., Owens, J. E., & Marsh, G. R. (1998). Binaural auditory beats affect vigilance performance and mood. *Physiology & Behavior*, 63(2), 249-252.

829 Le Scouarnec, R.-P., Poirier, R.-M., Owens, J. E., & Gauthier, J. (2001). Use of binaural beat tapes for
830 treatment of anxiety: a pilot study of tape preference and outcomes. *Alternative Therapies*
831 *in Health and Medicine*, 7(1), 58.
832 Lee, T. W., Girolami, M., Bell, A. J., & Sejnowski, T. J. (2000). A unifying information-theoretic
833 framework for independent component analysis. *Computers & Mathematics with*
834 *Applications*, 39(11), 1-21.
835 Lehmann, A., & Schönwiesner, M. (2014). Selective attention modulates human auditory brainstem
836 responses: relative contributions of frequency and spatial cues. *PLOS ONE*, 9(1), e85442.
837 Licklider, J. C. R., Webster, J. C., & Hedlun, J. M. (1950). On the frequency limits of binaural beats.
838 The Journal of the Acoustical Society of America, 22(4), 468-473.
839 Lins, O. G., & Picton, T. W. (1995). Auditory steady-state responses to multiple simultaneous
840 stimuli. Electroencephalography and Clinical Neurophysiology/Evoked Potentials Section,
841 96(5), 420-432.
842 Lisman, J. E., & Jensen, O. (2013). The Theta-Gamma Neural Code. *Neuron*, 77(6), 1002–1016.
843 https://doi.org/10.1016/j.neuron.2013.03.007
844 López-Caballero, F., & Escera, C. (2017). Binaural beat: a failure to enhance EEG power and
845 emotional arousal. *Frontiers in Human Neuroscience*, 11, 557.

Mammarella, N., Fairfield, B., & Cornoldi, C. (2007). Does music enhance cognitive performance in healthy older adults? The Vivaldi effect. Aging clinical and experimental research, 19(5), 394-399.

Maris, E., & Oostenveld, R. (2007). Nonparametric statistical testing of EEG- and MEG-data. *Journal of Neuroscience Methods*, 164(1), 177–190. https://doi.org/10.1016/j.jneumeth.2007.03.024

McIntosh, A. R., & Mišić, B. (2013). Multivariate statistical analyses for neuroimaging data. *Annual Review of Psychology*, 64, 499-525.

Moore, B. C. J. (2012). An introduction to the psychology of hearing (6th edn.). London: Brill.

Nolte, G., Bai, O., Wheaton, L., Mari, Z., Vorbach, S., & Hallett, M. (2004). Identifying true brain interaction from EEG data using the imaginary part of coherency. *Clinical Neurophysiology*, 115(10), 2292-2307.

Nozaradan, S., Schönwiesner, M., Caron-Desrochers, L., & Lehmann, A. (2016). Enhanced brainstem and cortical encoding of sound during synchronized movement. Neuroimage, 142, 231-240.

Ortiz, T., Martínez, A. M., Fernández, A., Maestu, F., Campo, P., Hornero, R., … Poch, J. (2008). Impact of auditory stimulation at a frequency of 5 Hz in verbal memory. Actas Espanolas De Psiquiatria, 36(6), 307–313.

863 Osipova, D., Takashima, A., Oostenveld, R., Fernández, G., Maris, E., & Jensen, O. (2006). Theta and
864 gamma oscillations predict encoding and retrieval of declarative memory. *Journal of*
865 *Neuroscience*, 26(28), 7523-7531.
866 Oster, G. (1973). Auditory beats in the brain. *Scientific American*, 229(4), 94-103.
867 Padmanabhan, R., Hildreth, A. J., & Laws, D. (2005). A prospective, randomised, controlled study
868 examining binaural beat audio and pre-operative anxiety in patients undergoing general
869 anaesthesia for day case surgery. *Anaesthesia*, 60(9), 874-877.
870 Perrott, D. R., & Nelson, M. A. (1969). Limits for the detection of binaural beats. The journal of the
871 Acoustical Society of America, 46(6B), 1477-1481.
872 Picton, T. W., John, M. S., Dimitrijevic, A., & Purcell, D. (2003). Human auditory steady-state
873 responses: Respuestas auditivas de estado estable en humanos. International journal of
874 audiology, 42(4), 177-219.
875 Picton, T. W., van Roon, P., & John, M. S. (2007). Human auditory steady-state responses during
876 sweeps of intensity. Ear and Hearing, 28(4), 542-557.
877 Pratt, H., Starr, A., Michalewski, H. J., Dimitrijevic, A., Bleich, N., & Mittelman, N. (2010). A
878 comparison of auditory evoked potentials to acoustic beats and to binaural beats. Hearing
879 Research, 262(1), 34–44.

880 Rainville, P., Hofbauer, R. K., Bushnell, M. C., Duncan, G. H., & Price, D. D. (2002). Hypnosis
881 modulates activity in brain structures involved in the regulation of consciousness. *Journal*
882 *of Cognitive Neuroscience*, 14(6), 887–901.http://doi.org/10.1162/089892902760191117
883 Reedijk, S. A., Bolders, A., Colzato, L. S., & Hommel, B. (2015). Eliminating the Attentional Blink
884 through Binaural Beats: A Case for Tailored Cognitive Enhancement. *Frontiers in Psychiatry*,
885 *6*. https://doi.org/10.3389/fpsyt.2015.00082
886 Reedijk, S. A., Bolders, A., & Hommel, B. (2013). The impact of binaural beats on creativity.
887 *Frontiers in Human Neuroscience*, 7:786. doi: 10.3389/fnhum.2013.00786
888 Rhodes, L. (1993). Use of the Hemi-Sync super sleep tape with a preschool-aged child. *Hemi-Sync*
889 *Journal, XI (4), pp. iv-v.*
890 Ross, B., Borgmann, C., Draganova, R., Roberts, L. E., & Pantev, C. (2000). A high-precision
891 magnetoencephalographic study of human auditory steady-state responses to amplitude-
892 modulated tones. The Journal of the Acoustical Society of America, 108(2), 679-691.
893 Ross, B., Miyazaki, T., Thompson, J., Jamali, S., & Fujioka, T. (2014). Human cortical responses to
894 slow and fast binaural beats reveal multiple mechanisms of binaural hearing. *Journal of*
895 *Neurophysiology*, *112*(8), 1871–1884. https://doi.org/10.1152/jn.00224.2014

Santarelli, R., Scimemi, P., Dal Monte, E., & Arslan, E. (2006). Cochlear microphonic potential recorded by transtympanic electrocochleography in normally-hearing and hearing-impaired ears. Acta otorhinolaryngologica italica, 26(2), 78.

Schellenberg, E. G., Nakata, T., Hunter, P. G., & Tamoto, S. (2007). Exposure to music and cognitive performance: Tests of children and adults. Psychology of music, 35(1), 5-19.

Skoe, E., & Kraus, N. (2010). Auditory brainstem response to complex sounds: a tutorial. *Ear and Hearing*, 31(3), 302.

Solcà, M., Mottaz, A., & Guggisberg, A. G. (2016). Binaural beats increase interhemispheric alpha-band coherence between auditory cortices. *Hearing Research*, *332*, 233–237. https://doi.org/10.1016/j.heares.2015.09.011

Schwarz, D. W. F., & Taylor, P. (2005). Human auditory steady state responses to binaural and monaural beats. *Clinical Neurophysiology*, 116(3), 658–668. http://doi.org/10.1016/j.clinph.2004.09.014

Takahashi, T., Murata, T., Hamada, T., Omori, M., Kosaka, H., Kikuchi, M., ... & Wada, Y. (2005). Changes in EEG and autonomic nervous activity during meditation and their association with personality traits. *International Journal of Psychophysiology*, 55(2), 199-207.

Tarr, B., Launay, J., & Dunbar, R. I. (2014). Music and social bonding: "self-other" merging and neurohormonal mechanisms. Frontiers in psychology, 5, 1096.

914 Varela, F., Lachaux, J. P., Rodriguez, E., & Martinerie, J. (2001). The brainweb: phase
915 synchronization and large-scale integration. *Nature Reviews in Neuroscience*, 2(4), 229.
916 Van Eeckhoutte, M., Wouters, J., & Francart, T. (2016). Auditory steady-state responses as neural
917 correlates of loudness growth. *Hearing Research*, 342, 58-68.
918 Wahbeh, H., Calabrese, C., & Zwickey, H. (2007). Binaural Beat Technology in Humans: A Pilot
919 Study To Assess Psychologic and Physiologic Effects. *The Journal of Alternative and*
920 *Complementary Medicine*, 13(1), 25–32. https://doi.org/10.1089/acm.2006.6196
921 Wernick, J. S., & Starr, A. (1968). Binaural interaction in the superior olivary complex of the cat: an
922 analysis of field potentials evoked by binaural-beat stimuli. *Journal of Neurophysiology*,
923 31(3), 428-441.
924 Yamsaard, T., & Wongsawat, Y. (2014). The relationship between EEG and binaural beat
925 stimulation in meditation. In *Biomedical Engineering International Conference (BMEiCON),*
926 *2014 7th* (pp. 1–4). IEEE.
927 Zampi, D. D. (2015). Efficacy of Theta-Binaural Beats for the Treatment of Chronic Pain.
928 Northcentral University.

929 # Tables

	Data Structure	Statistical Test	C.I.
a	Not normal (W=0.9, p=0.0001)	Permutation One-Way repeated measures ANOVA	0.13, 3.04
b	Normal (W=0.96, p=0.013)	Permutation One-Way repeated measures ANOVA	0.09, 3.08
c	Normal (W=0.99, p=0.86)	Permutation Factorial (2x2) repeated measures ANOVA	
		Frequency	0.001, 5.6
		Beat type	0.002, 5.99
		Interaction	0.001, 5.67
d	Not normal (W=0.96, p=0.05)	Permutation Factorial (2x2) repeated measures ANOVA	
		Frequency	0.001, 5.46
		Beat type	0.001, 6.1
		Interaction	0.0003, 5.45
e	Not normal (W=0.492,	Permutation Factorial (2x2) repeated	

	p=1.549e-13)	measures ANOVA		
			Frequency	0.001, 6.31
			Beat type	0.001, 6.66
			Interaction	0.001, 6.43
f	Not normal (W=0.625,	Permutation Factorial (2x2) repeated		
	p=1.631e-11)	measures ANOVA		
			Frequency	0.001, 7.1
			Beat type	0.001, 7.68
			Interaction	0.001, 6.26
		Post-hoc permutation paired t-test		-2.02, 2.39
		(Monaural Gamma vs Monaural Theta)		
		Post-hoc permutation paired t-test		-2.4, 2.23
		(Binaural Gamma vs Monaural Gamma)		
		Post-hoc permutation paired t-test		-2.1, 2
		(Binaural Gamma vs Binaural)		
g	Spatial-spectral-temporal	Non-parametric, cluster-based		
	(Hilbert Transform)	permutation tests		
			Monaural Gamma vs Baseline at 40 Hz	0.57, 4.07

h	Spatial-spectral-temporal (PLV)	Non-parametric, cluster-based permutation tests	
		Binaural Theta vs Monaural Theta at 40 Hz	2.55, 5.99
			2.02, 6.04
		Binaural Gamma vs Monaural Gamma at alpha	2.5, 6.11
		Binaural Gamma vs Monaural Gamma at Gamma	2.5, 6.11
		Binaural Gamma vs Monaural Gamma at Gamma	2.69, 6.62
		Binaural Gamma vs Monaural Gamma at 40 Hz	2.79, 6.99
		Monaural Gamma vs Baseline at 40 Hz	
i	Spatial-spectral-temporal (Fourier Transform)	Non-parametric, cluster-based permutation tests	
		Binaural Theta vs Baseline at theta	0.85, 4.89

		Binaural Theta vs Baseline at 40 Hz	-1.39, 4.06
j	Spatial-spectral-temporal (Neurophenomenological)	Non-parametric, cluster-based permutation tests	
		MR - Negative frontal cluster at theta	0.93, 3.25
		MR - Negative frontocentral to occipital at theta	3.2, 6.38
			2.54, 5.86
		MR - Negative frontal to right temporal occipital at 40 Hz	-1.45, 4.03
		AD - Negative right temporal at 40 Hz	

Table 1: Statistical Table. Description of statistical tests and confidence intervals for each of the results reported on the main text.

Figures and legends

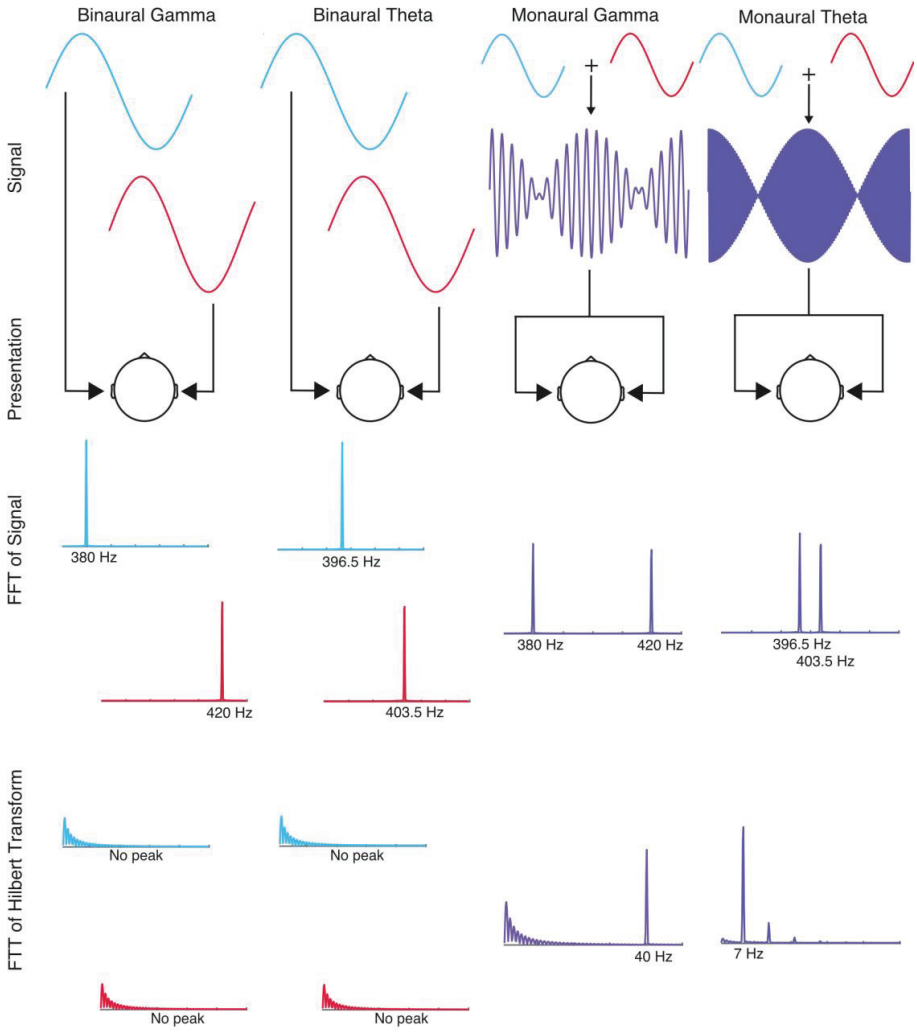

Figure 1. Beats: Signal, Presentation method, Fast Fourier Transform (FFT) and FFT of Hilbert Figure Transform. Each column represents one experimental condition. **(Signal and Presentation rows)** Binaural beats are created by dichotically presenting two pure tones with a slight frequency mismatch (Red color = right ear). Monaural beats are created by digitally summing these tones and presenting the resulting signal diotically. **(FFT of Signal)** Stimuli were analyzed using a Fourier transform to obtain their frequency composition. **(FFT of Hilbert Transform)** The FFT of

the Hilbert transform (i.e. the analytic signal) was computed to tap into the spectral information of the envelope of the signal (the beat frequency). The frequency of the envelope of the summed tones encodes beat frequency (e.g. 403.5 - 396.5 = 7 Hz for Theta). This information, however, is only encoded in monaural beats because they are digitally summed.

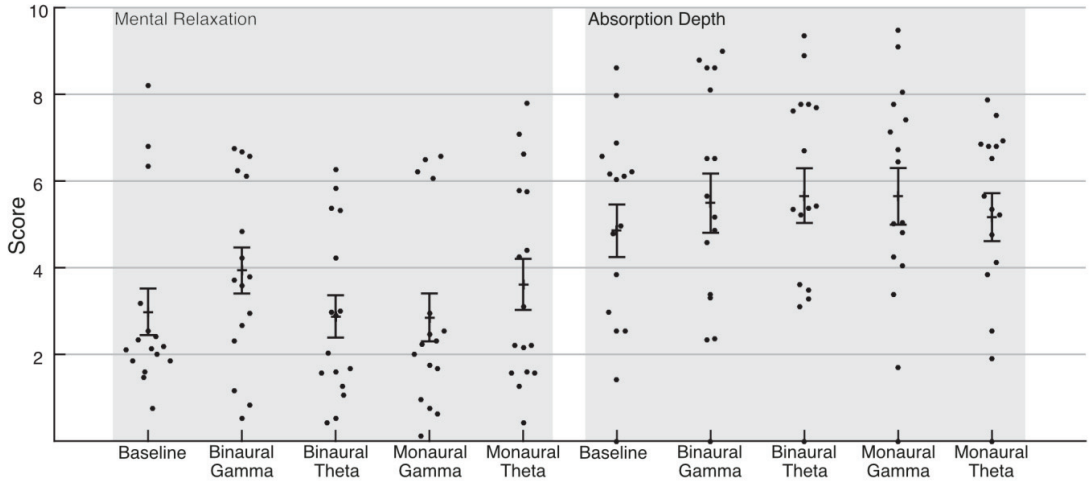

Figure 2. Visual Analogue Scales: Mental relaxation and absorption depth. Each data point represents one participant' s self-reported score. Mean is plotted as a black horizontal line ± standard error of the mean.

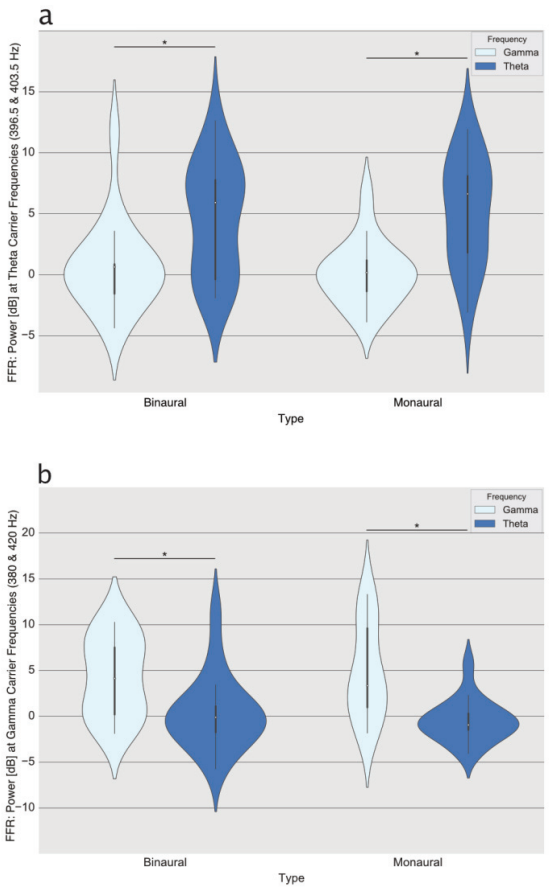

977
978
979

980 **Figure 3. Frequency Following Response (FFR) to carrier pure tones.** Plotted here: violin plots
981 with median (white dots), quartile (thick black line) and whisker (thin black line) values. Please
982 note the scale is decibel change from baseline, a logarithmic scale where each 3 dBs represent a
983 difference of a factor of 2. Each violin plot represents all participants' baseline-normalized (dB)
984 averages of the power around a 1 Hz bin (e.g. 396.5 ± 0.5 Hz) at beat carrier frequencies (e.g.
985 396.5 and 403.5 Hz were averaged together for theta conditions). This power was obtained from
986 the average activity at all channels of each participant. Asterisks above lines linking conditions
987 denote a significant difference between them ($p < 0.05$). **(a)** Frequency Following Response
988 elicited at theta-carrier frequencies (average of 396.5 and 403.5 Hz). **(b)** Frequency Following
989 Response elicited at gamma-carrier frequencies (average of 380 and 420 Hz).

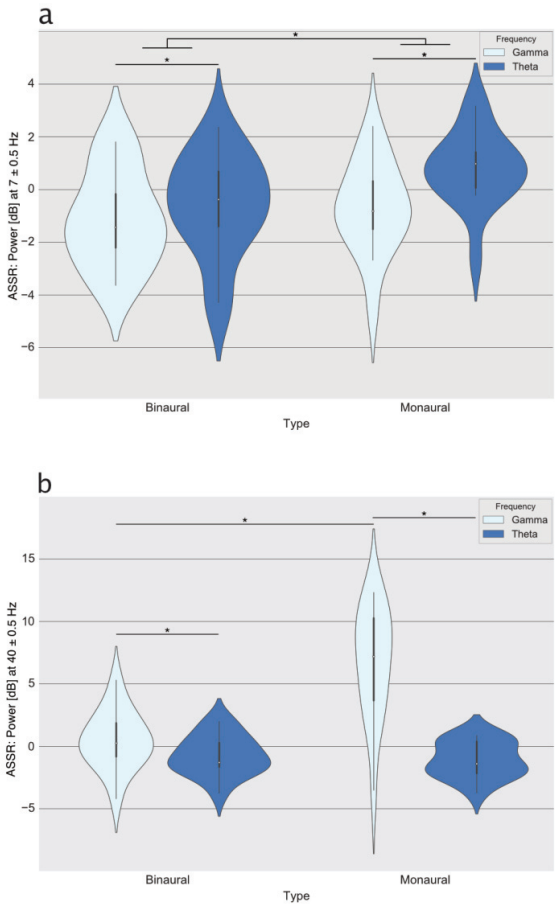

Figure 4. Auditory Steady State Responses (ASSR) to beat frequency. Plotted here: violin plots with median (white dots), quartile (thick black line) and whisker (thin black line) values. Please note the scale is decibel change from baseline, a logarithmic scale where each 3 dBs represent a difference of a factor of 2. Each violin plot represents all participants' baseline-normalized (dB) averages of the power around a 1 Hz bin (e.g. 7 ± 0.5 Hz) at beat frequencies (either 7 or 40 Hz) obtained from the average activity at all channels for each participant. Asterisks above lines linking conditions denote a significant difference between them ($p < 0.05$). Please note that there was an outlier in these graphs that was taken out for visualization purposes (a participant with data points at around -30 dB). **(a)** Cortical activity elicited at 7 Hz. **(b)** Cortical activity elicited at 40 Hz.

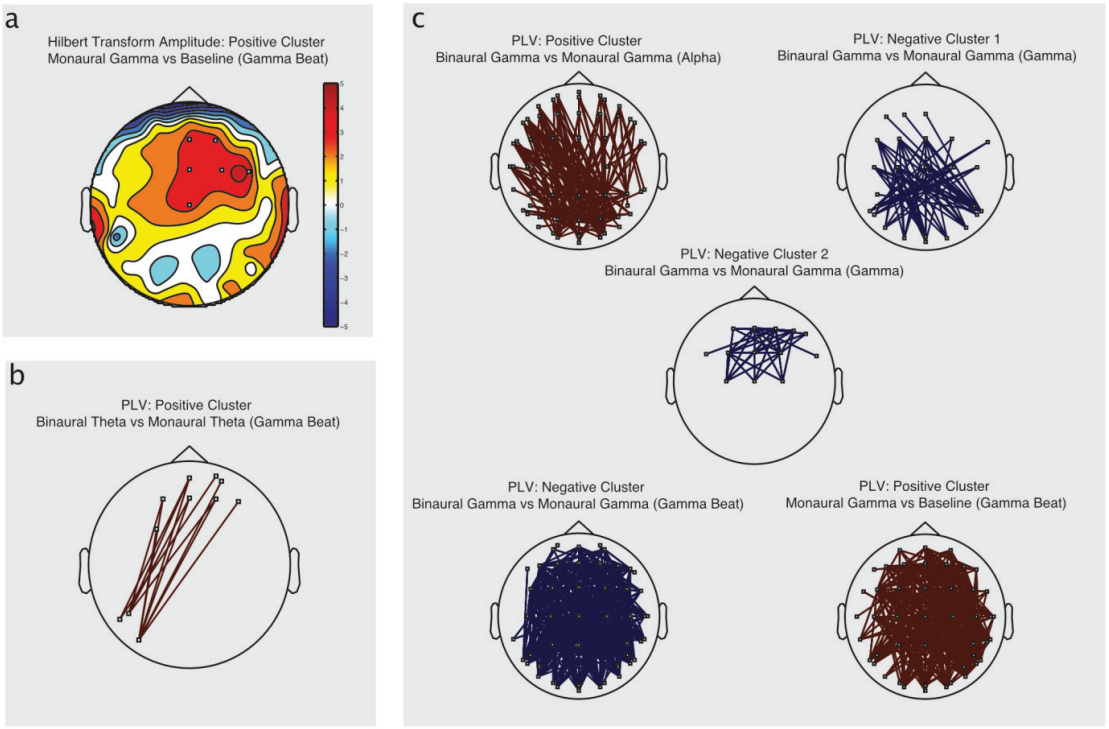

Figure 5. Contrast topographies for Phase-locking value (PLV) and Hilbert Transform amplitude. Topographies were averaged across participants and compared to either baseline or between beat type (binaural vs monaural). Both statistics (Hilbert Transform Amplitude and PLV) were normalized using z scores. We only show contrasts that exhibit at least three significant electrodes (depicted as small white squares). Frequency band limits are as follows: Delta (1 - 4 Hz), Theta (5 - 8 Hz), Alpha (9 - 12 Hz), Beta (13 - 30 Hz), Gamma (32 - 48 Hz), Theta Beat (6 - 8 Hz) and Gamma Beat (39 - 41 Hz). **(a) Hilbert transform amplitude used as a local synchronization**

index. The color bar indicates T-values from student' s test. **(b) Phase locking value used as an index of long-distance synchronization between electrodes during theta conditions.** Red lines indicate a significant positive phase locking value (PLV) between two electrodes. **(c) Phase locking value used as an index of long-distance synchronization between electrodes during gamma conditions.** Red lines indicate a significant positive phase locking value (PLV) between two electrodes while blue lines indicate a negative one.

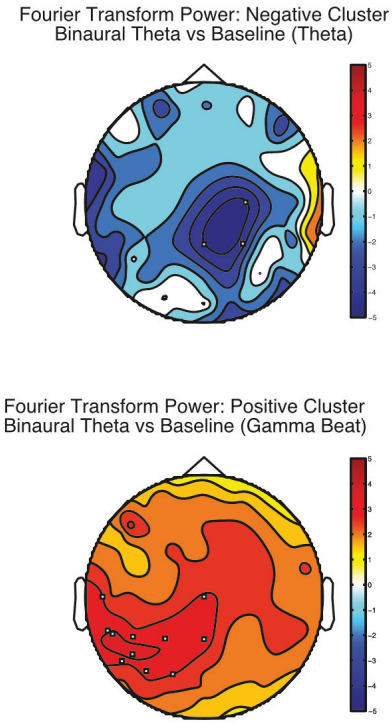

Figure 6. Fourier transform power used as a local synchronization index in Theta conditions. Topographies were averaged across participants and compared to baseline. Fourier Transform Power was normalized using z scores. We only show contrasts that exhibit at least three significant electrodes (depicted as small white squares). Frequency band limits are as follows: Delta (1 - 4 Hz), Theta (5 - 8 Hz), Alpha (9 - 12 Hz), Beta (13 - 30 Hz), Gamma (32 - 48 Hz), Theta Beat (6 - 8 Hz)

and Gamma Beat (39 - 41 Hz). The color bar indicates T-values from student' s test. Please note that no iCOH contrasts were significant.

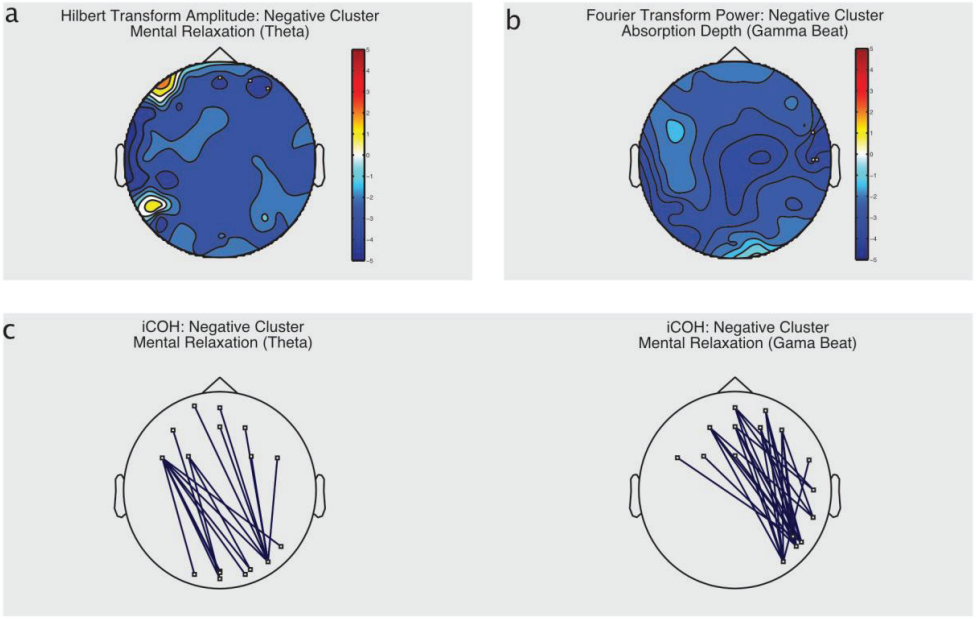

Figure 7. Neurophenomenological analysis: correlates between subjective experience and EEG connectivity patterns. Each participants' two highest rated (Mental Relaxation and Absorption Depth) experimental conditions (binaural gamma, monaural theta…) were contrasted with the two lowest rated conditions. These contrasts were then averaged across participants for each separate scale (Mental Relaxation and Absorption Depth). All statistics were normalized

using z scores. We only show contrasts that exhibit at least three significant electrodes here (depicted as small white squares). Frequency band limits are as follows: Delta (1 - 4 Hz), Theta (5 - 8 Hz), Alpha (9 - 12 Hz), Beta (13 - 30 Hz), Gamma (32 - 48 Hz), Theta Beat (6 - 8 Hz) and Gamma Beat (39 - 41 Hz). **(a) Hilbert transform amplitude used as a local synchronization index.** The color bar indicates T-values from student' s test. **(b) Fourier transform power used as a local synchronization index.** The color bar indicates T-values from student' s test. **(c) Imaginary Coherence used as an index of long-distance synchronization between electrodes.** Blue lines indicate a significant negative iCOH between two electrodes.